



Development and Characterization of Fe-Si-Cu-Nb-B Nanocrystalline Alloy Applied in High Performance Magnetic Sensors

G. Perez¹, L. C. C. Benyosef², A. Wiermann³, I. G. Solorzano⁴,

Lecturer, Nanotechnology Coordination, Federal University of Rio de Janeiro (UFRJ), Duque de Caxias - RJ, Brazil¹

Researcher, Materials Metrology Division, National Institute of Metrology Quality and Technology (Inmetro), Duque de Caxias, RJ, Brazil¹

Full Professor, Coordination of Geophysics, Observatório Nacional (ON), Rio de Janeiro, RJ, Brazil²

Researcher, Coordination of Geophysics, Observatório Nacional (ON), Rio de Janeiro, RJ, Brazil³

Associate Professor, Department of Materials Engineering, Pontifical Catholic University (PUC-Rio), Rio de Janeiro, RJ, Brazil⁴

ABSTRACT: Fluxgate sensors for application in magnetometers were built in the Magnetic Sensor Development Laboratory on the Observatório Nacional (LDSM/ON). To build the sensors, $\text{Fe}_{74.3}\text{Si}_{14.2}\text{Cu}_1\text{Nb}_3\text{B}_{7.5}$ alloy ribbons were produced by the melt-spinning technique. The amorphous ribbons were annealed at 554 °C for 1 h to form the α -Fe(Si) nanocrystalline phase embedded in an intergranular amorphous phase. Before building the fluxgate sensor cores, the materials were subjected to structural, thermal and magnetic characterization. The formation of amorphous and nanocrystalline structures were verified by x-ray diffraction (XRD) and transmission electron microscopy (TEM) on the as spun and annealed samples respectively. The magnetic properties of the ribbons were analyzed by vibrating sample magnetometer (VSM) and by circuit of coils at different frequencies. Finally, the developed nanocrystalline sensors core were submitted to a test in an open fluxgate circuit and these results were compared with others from amorphous sensors core built using Co-Fe-Si-B ribbons.

KEYWORDS: Fluxgate magnetometer, magnetic sensors, nanocrystalline alloys, Instrumentation.

I. INTRODUCTION

Since 1940's Permalloy and ferrite was used in the core of the first magnetometers [1]. Then, around 1980's, an amorphous Co based alloy has been introduced as magnetic sensors [2]. Practically in the same period a new family of alloys Fe-Si-B-Cu-Nb, also known as FINEMET, had been developed in 1988 by Yoshizawa et al [3]. This family showed excellent soft magnetic properties for magnetic sensors applications [4]. All these alloys combine both high permeability and high saturation.

Fe-Si-B-Cu-Nb alloy has a nanocrystalline structure composed of body centered cubic (bcc) Fe-Si supersaturated solution [3], the α -Fe(Si) phase, embedded in the remaining amorphous matrix [5]. The composition of these nanograins or nanocrystals is around Fe_3Si , which result on DO_3 order [6]. The size of the DO_3 order region and the degree of order of the α -Fe(Si) phase increase with increasing annealing temperature and the local content of Si into bcc nanograins is bigger than the mean content of alloy [7]. These nanostructures are obtained by annealing (at 550 °C) of the melt-spun amorphous ribbons [3].

Several mechanisms occur during annealing process: at the initial stage the copper diffusion through amorphous matrix produce the formation of small Cu rich clusters randomly dispersed. These Cu clusters works as catalyst of the α -Fe(Si) nucleation [7-10], which is only possible with niobium addition [6, 11, 12]. These Cu clusters continue to grow during the crystallization process until reaching the size around of 5 nm [8]. The nucleation of Fe-Si nanocrystals occurs adjacent to Cu clusters, while the Fe-Si structure tends to reject Cu to the remaining amorphous



International Journal of Advanced Research in Electrical, Electronics and Instrumentation Engineering

(An ISO 3297: 2007 Certified Organization)

Website: www.ijareeie.com

Vol. 6, Issue 6, June 2017

phase as it grows, thus, limiting the rate of coarsening of the initial Cu clusters. During the next stage, Fe-Si nanocrystals growth, the niobium is rejected out of the crystalline structure, kept in the crystalline-amorphous matrix interface, so the nanocrystal is involved by a niobium shell, becoming a diffusional barrier to prevent the growth of Fe-Si nanocrystals [10]. In the final stages of the annealing there are three phases: small Cu clusters with less than 5 nm of diameter, α -Fe(Si) nanocrystals of approximated composition Fe_3Si and amorphous remaining phase containing 10-15 % of Nb and B [10].

Each element has a role in the alloy. The pure iron is a ferromagnetic material; it has a high saturation and permeability. The additional elements produce a decreasing in magnetic saturation, but improve other magnetic properties. The silicon presence in the alloy decreases a little bit the saturation, but raises the electrical resistivity, reducing eddy currents, also lowering the magnetostriction, the magnetic anisotropy and the coercivity. Others works have shown that this alloy with around 15 % atomic of Si presents values of magnetostriction near zero [6]. The copper is the catalyst for the nucleation of the nanocrystals. It was shown that alloys with 1% of Cu presents a homogeneous distribution of nanocrystals [10]. The main effect of niobium is to inhibit the nanocrystals growth during the annealing. Previous works show that alloys of high content of Nb present smaller size of crystals than alloys of low or without any content of Nb [11]. The Nb is a stabilizer of amorphous face [13] and changes the Cu solubilization, thus promoting a finer nanoclusters distribution [10]. The boron assists the niobium to inhibit the growth of nanocrystals [14].

Some attention on important details must be taken during amorphous ribbons production by melt-spinning: The speed of the wheel is one of the main factors to control the cooling rate and the thickness of the obtained ribbon [15]. As the speed is increased, the melted material is dragged more rapidly, avoiding its accumulation, which results in a reduction of thickness, with consequent increase in the cooling rate thus promoting the formation of an amorphous structure. The volumetric flow rate is controlled by the ejecting pressure, which is directly related with the thickness of the obtained ribbon. The width of the ribbon is controlled by the crucible hole diameter [16]. It is very important that the surface of the copper wheel be very well polished in order to reduce the roughness on the ribbon surface.

II. EXPERIMENTAL

Ribbons Production

The $Fe_{74.3}Si_{14.2}Cu_1Nb_3B_{7.5}$ alloy ingot was prepared from 99.99 % pure materials using a plasma arc furnace under argon atmosphere. The ingot was remelted in a quartz crucible in an Edmund Buehler GmbH melt-spinner's induction furnace. To ensure homogeneity, the melted alloy was kept at 1400 °C for 10 min [11].

To produce the amorphous ribbons, the melt-spinner was set with the follow parameters: A quartz crucible with an orifice of 1.7 mm diameter; the distance between wheel and crucible was 0.3 mm. The ejection temperature was 1350 °C (almost 200 °C above the melting point of the alloy). The wheel speed was 48 m/s, the pressure in the crucible 100 mbar, and the chamber pressure was 20 mbar. The obtained amorphous ribbons had a thickness of 40 μ m and 1.8 mm width. Table 1 lists these parameters used in the production of the amorphous ribbons. During ribbon production, a decrease in ejection pressure with an increase in wheel speed leads to a higher cooling rate, thus ensuring the formation of the amorphous structure.

Table 1 - Parameters of the melt spinner and characteristics of the ribbons: Diameter of the crucible orifice (d_c), camera pressure (P_c), ejection pressure (P_e), wheel speed (V), crucible-to-wheel distance (Z), ejection temperature (T), ribbon thickness (t), and ribbon width (L).

| d_c (mm) | P_c (mbar) | P_e (mbar) | V (m/s) | Z (mm) | T (°C) | t (μ m) | L (mm) |
|------------|--------------|--------------|-----------|----------|----------|----------------|----------|
| 1.7 | 20 | 100 | 48 | 0.3 | 1350 | 40 | 1.8 |

Annealing

The amorphous ribbons were annealed in an electric furnace at a heating rate of 10 °C/min and kept at 554 °C for 1 h in N_2 atmosphere. The ribbons were cooled by thermal inertia of the furnace.

International Journal of Advanced Research in Electrical, Electronics and Instrumentation Engineering

(An ISO 3297: 2007 Certified Organization)

Website: www.ijareeie.com

Vol. 6, Issue 6, June 2017

Structural characterization

The structures of the as-spun (amorphous) and annealed sample (nanocrystalline) were characterized by x-ray diffraction (XRD) and then observed by transmission electron microscopy (TEM). A Shimadzu 2000 x-ray diffractometer using Cu-K_α radiation ($\lambda=1.5418 \text{ \AA}$) and a Jeol 2010 instrument, operating at 200 kV under diffraction and phase contrast modes, were used respectively. To prepare a TEM sample, a piece of each ribbon, previously dimpled by 656 Gatan Dimple Grinder, were bonded to a 3 mm diameter slotted copper grid, then a Gatan DuoMill 600 ion milling was used to produce a hole of sharp edges in the TEM samples.

Magnetic characterization

Magnetic properties of these samples, at room temperature, were measured using a Quantum Design Versalab, 3 Tesla, Cryogen-free vibrating sample magnetometer (VSM).

Dynamic magnetic properties of the as-spun and annealed samples were measured at frequencies from 100 Hz to 10.0 kHz, using a specially developed hysteresimeter for small ribbon samples.

Sensor construction

Our experiments have shown that the ribbons (nanocrystalline) become very brittle after annealing [17], probably due to segregation of boron and the formation of intergranular borates [12]. Therefore, to avoid handling such fragile material, the amorphous Fe_{74.3}Si_{14.2}Cu₁Nb₃B_{7.5} ribbons were rolled up inside a metallic ring core support which was then inserted into the furnace for annealing at 540 °C for 1 h. The ring core support was made of a special non magnetic brass.

After annealing, the ring core was rolled up by the primary coil and inserted in the secondary coil, which was made of polystyrene with 400 turns of enameled copper wire. An open circuit fluxgate was built to test the sensor cores.

Sensor test

A Helmholtz coil with a field/current ratio of 170 nT/mA was used to generate test fields to exercise the sensors. The sensor core was centered into the Helmholtz coils, as illustrated in Fig 1, while the results are depicted in Fig 9. The noise level [18, 19] was estimated from a linear fitting analysis, the combined effect of noise and non-linearity produce dispersion in points of the characteristic curve of the magnetometer. The core was tested in magnetic fields spanning from $\square 150,000$ to +150,000 nT (almost five times that of the Earth's field). A fluxgate sensor amorphous core with a nominal composition of Co_{66.5}Fe_{3.5}Si₁₂B₁₈, produced in the LDSM/ON, was used as comparison. The ribbons of this sensor have been subjected to stress annealing.

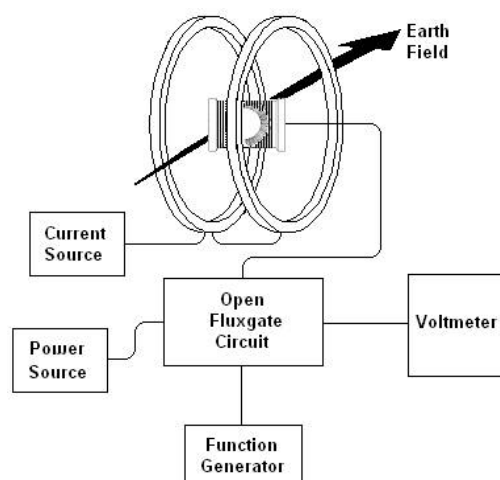


Fig .1 Circuit array for sensor test of linearity measurements

III.RESULTS

Structural characterization

Fig 2 shows two X-ray diffractograms of the samples, one before and the other after annealing. The as-spun sample presents a typical diffractogram for amorphous structure (below), while the annealed sample shows the typical peaks of the crystalline nanostructure (above).

The lattice parameter of the BCC phase is calculated to be 0.284 - 0.285 nm from the X-ray diffractometry, that corresponding to (200) plane of the DO₃ superlattice structure. The transmission electron microscopy results show an evidence of the formation of the DO₃ superlattice structure. Previous works indicates that a approximate composition of the nanocrystalline phase is Fe₃Si [20] of a complex bcc structure [17] forming DO₃ superlattice structure [21].

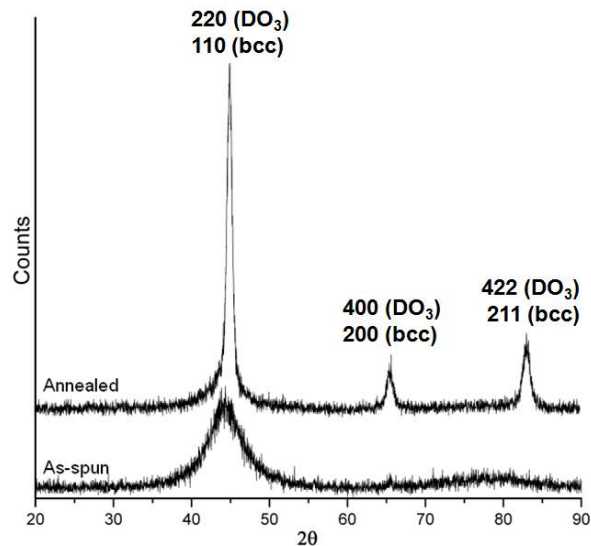


Fig .2 XRD patterns of material before and after annealing. The diffractogram of the as-spun sample (below) does not show peaks, typical of amorphous structures. The diffractogram of the annealed sample (above) shows peaks of the α -Fe(Si) crystalline phase.

The TEM micrograph, of Fig 3(a), shows the amorphous structure of the as-spun sample and its corresponding selected area diffraction pattern, Fig 3(b), which shows diffuse rings of amorphous materials, typical of amorphous structures. TEM images on Fig 4(c) confirm the formation of nanocrystalline phase in the annealed sample. Fig 4(c) show grains in the order of 10 nm. Polygonal and faceted shapes were not observed; most of nanocrystals have a spheroidal shape, indicating the presence of the remaining intergranular amorphous phase that have avoided the impingement between the grains during the growth stage. Fig 3(d) shows the electron diffraction pattern of the nanocrystalline sample, which shows typical sharp rings of nanocrystalline structure.

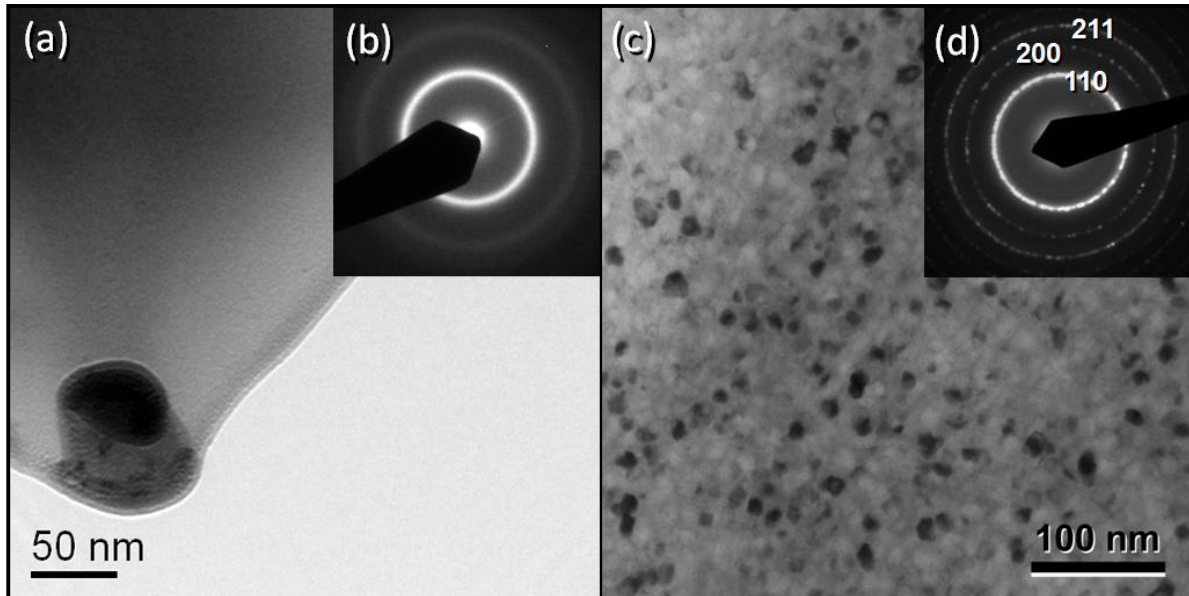


Fig .3 (a) TEM micrograph of amorphous structure of the as-spun sample, (b) inserted corresponding selected area electron diffraction pattern, diffuse rings can be observed, typical of amorphous structures, (c) TEM micrograph of annealed sample, (d) selected area electron diffraction pattern.

Magnetic characterization

The VSM results indicate the enhancement of the soft magnetic properties on the annealed samples. This enhancement in soft magnetic properties strongly depends on the changes of the microstructure and magnetic domain structure, occurring during annealing [6]. Magnetic hysteresis loops of the as-spun and annealed samples obtained by VSM, are shown in Fig 4. The loop of the annealed sample indicates higher magnetic permeability than the as-spun sample. Values of magnetic saturation around 120 Emu/g were recorded on the both samples. The values of coercivity and remanent magnetization can be considered near zero (coercivity below 1 Oe and remanent magnetization smaller than 2 Emu/g).

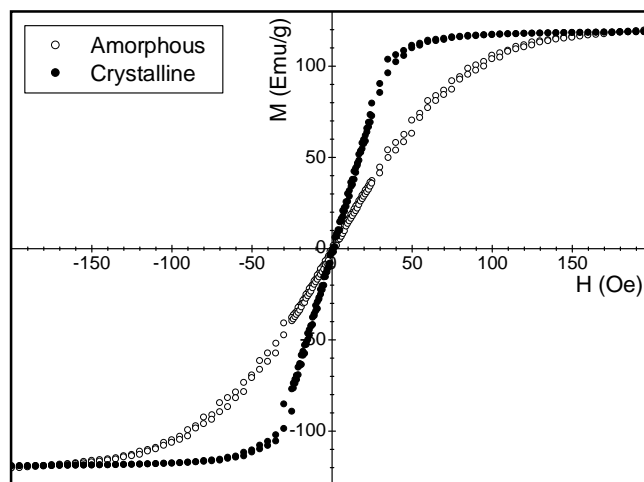


Fig .4 Hysteresis loops of as-spun and annealed samples measured by VSM.

International Journal of Advanced Research in Electrical, Electronics and Instrumentation Engineering

(An ISO 3297: 2007 Certified Organization)

Website: www.ijareeie.com

Vol. 6, Issue 6, June 2017

The dynamic magnetic measurement indicates that the annealed samples presented lower coercivity, higher magnetic saturation and higher permeability than as spun sample for all frequencies, while the best soft magnetic properties were presented for frequencies up to 5.0 kHz (Fig 5). It was observed that the increase in the frequency of the applied magnetic field produces a rise in coercivity.

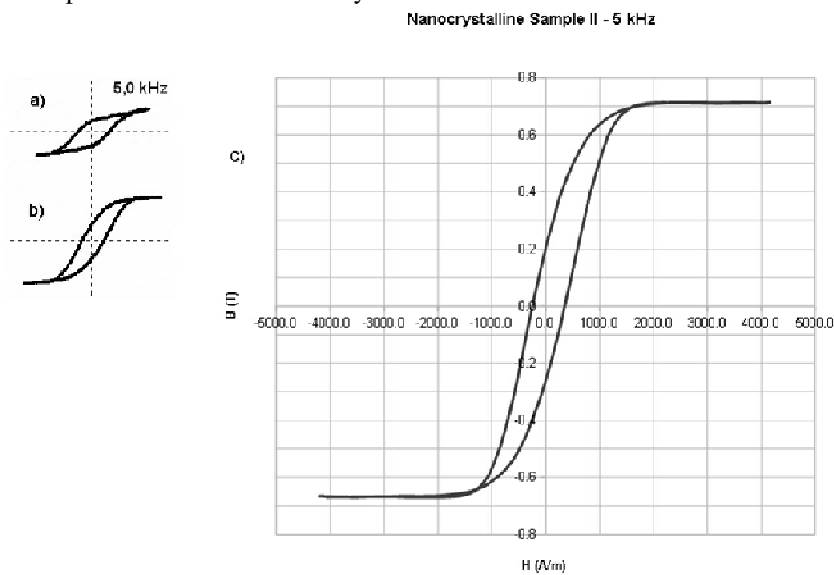


Fig .5 Low resolution (fast) B-H loops of (a) amorphous and (b) nanocrystalline $Fe_{74.3}Si_{14.2}Cu_1Nb_3B_{7.5}$ alloy at 5.0 kHz. In (c) a high resolution B-H loop at 5 kHz for the annealed sample is shown.

Sensor test

Test results of the annealed $Fe_{74.3}Si_{14.2}Cu_1Nb_3B_{7.5}$ alloy showed an excellent linearity in the entire operating band. The $Co_{66.5}Fe_{3.5}Si_{12}B_{18}$ amorphous core [22] was also tested (Fig 6) for purposes of results comparison with the nanocrystalline sensor. The annealed $Fe_{74.3}Si_{14.2}Cu_1Nb_3B_{7.5}$ alloy presents less scattering than the $Co_{66.5}Fe_{3.5}Si_{12}B_{18}$ amorphous alloy.

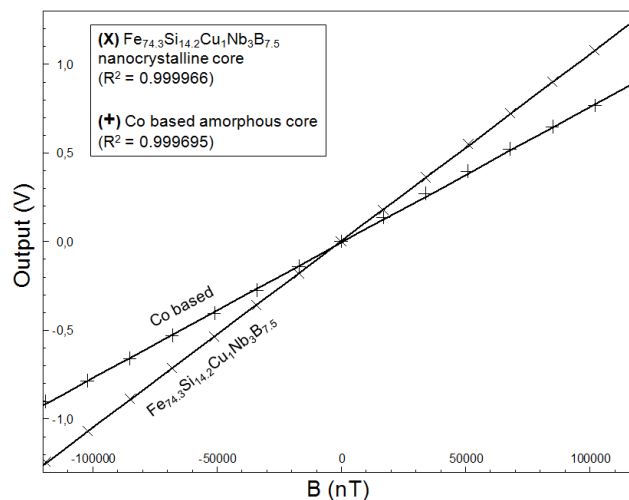


Fig .6 Results of linearity test of the nanocrystalline $Fe_{74.3}Si_{14.2}Cu_1Nb_3B_{7.5}$ sensor and amorphous cobalt base sensor.



International Journal of Advanced Research in Electrical, Electronics and Instrumentation Engineering

(An ISO 3297: 2007 Certified Organization)

Website: www.ijareeie.com

Vol. 6, Issue 6, June 2017

IV.CONCLUSIONS

Fe_{74.3}Si_{14.2}Cu₁Nb₃B_{7.5} alloy exhibit the DO₃ structure after annealing. The microstructure is uniform, composed of the DO₃ nanocrystals, surrounded by retained amorphous phase.

The annealed samples present nanocrystals of 10 nm homogeneous size distribution and have homogeneous distribution into the amorphous matrix. These nanocrystalline samples have shown excellent soft magnetic properties suitable for applications in fluxgate sensors.

Each alloy has its own particular frequency, this alloy showed low coercivity and high permeability at frequencies near of 5 kHz. The performance of the material declined as the frequency increased or decreased from this value. In the fabrication of sensors, care must be taken in handling the ring core and in the choice of geometric configuration of the ring core supports, since these features have considerable influence on the performance of the sensor.

It was found that cores made of these nanocrystalline materials showed a highly linear response with low scattering, making this material a promising option for building highly accurate fluxgate sensors.

ACKNOWLEDGMENTS

The authors acknowledge FAPERJ and CAPES (Brazil) for its partial funding of this project.

REFERENCES

- [1] L. C. d. C. Benyosef, G. C. Stael, and M. Bochner, "Optimization of the magnetic properties of materials for fluxgate sensors," *Materials Research*, vol. 11, pp. 145-149, 2008.
- [2] O. V. Nielsen, J. R. Petersen, A. Fernandez, B. Hernando, P. Spisak, F. Primdahl, *et al.*, "Analysis of a fluxgate magnetometer based on metallic glass sensors," *Measurement Science and Technology*, vol. 2, p. 435, 1991.
- [3] "New Fe \square based soft magnetic alloys composed of ultrafine grain structure," *Journal of Applied Physics*, vol. 64, pp. 6044-6046, 1988/11/15 1988.
- [4] O. V. Nielsen, J. R. Petersen, and G. Herzer, "Temperature dependence of the magnetostriction and the induced anisotropy in nanocrystalline FeCuNbSiB alloys, and their fluxgate properties," *IEEE Transactions on Magnetics*, vol. 30, pp. 1042-1044, 1994.
- [5] W. Lefebvre, S. Morin-Grognet, and F. Danoix, "Role of Niobium in the nanocrystallization of a Fe_{73.5}Si_{13.5}B₉Nb₃Cu alloy," *Journal of Magnetism and Magnetic Materials*, vol. 301, pp. 343-351, 6// 2006.
- [6] K. H. J. Buschow, "Preface to volume 10," in *Handbook of Magnetic Materials*. vol. Volume 10, ed: Elsevier, 1997, pp. v-vii.
- [7] X. Y. Zhang, J. W. Zhang, F. R. Xiao, J. H. Liu, R. P. Liu, J. H. Zhao, *et al.*, "Ordering of the crystalline phase α -Fe(Si) in annealed Fe_{73.5}Cu₁Nb₃Si_{13.5}B₉ alloy," *Materials Letters*, vol. 34, pp. 85-89, 1998/02/01 1998.
- [8] P. Allia, P. Tiberto, M. Baricco, M. Knobel, and F. Vinai, "Nanostructured materials for soft magnetic applications produced by fast dc Joule heating," *IEEE Transactions on Magnetics*, vol. 30, pp. 4797-4799, 1994.
- [9] M. E. McHenry, F. Johnson, H. Okumura, T. Ohkubo, V. R. V. Ramanan, and D. E. Laughlin, "The kinetics of nanocrystallization and microstructural observations in FINEMET, NANOPERM and HITPERM nanocomposite magnetic materials," *Scripta Materialia*, vol. 48, pp. 881-887, 2003.
- [10] "On the role of Cu and Nb in the formation of nanocrystals in amorphous Fe_{73.5}Nb₃Cu₁Si_{13.5}B₉," *Applied Physics Letters*, vol. 64, pp. 974-976, 1994/02/21 1994.
- [11] N. A. Mariano, J. E. May, and S. E. Kuri, "Ligas Finemet nanocristalizadas a partir de precursores amorfos," *Rem: Revista Escola de Minas*, vol. 57, pp. 129-133, 2004.
- [12] A. O. Olofinjana and H. A. Davies, "Preparation and mechanical properties of Fe-Si-B-Nb-Cu nanocrystalline alloy wire," *Nanostructured Materials*, vol. 6, pp. 465-468, 1995/01/01 1995.
- [13] D. S. dos Santos and D. R. dos Santos, "Crystallization kinetics of Fe-B-Si metallic glasses," *Journal of Non-Crystalline Solids*, vol. 304, pp. 56-63, 6// 2002.
- [14] W. Gawior, M. Woch, R. Kolano, and N. Wójcik, "The structure and magnetic properties of Fe_{82.5-x}Cu₁Nb₃Si_{13.5}B_x alloys," *Journal of Magnetism and Magnetic Materials*, vol. 157, pp. 207-208, 1996/05/02 1996.
- [15] V. I. Tkatch, A. I. Limanovskii, S. N. Denisenko, and S. G. Rassolov, "The effect of the melt-spinning processing parameters on the rate of cooling," *Materials Science and Engineering: A*, vol. 323, pp. 91-96, 1/31/ 2002.
- [16] G. Pozo López, L. M. Fabietti, A. M. Condó, and S. E. Urreta, "Microstructure and soft magnetic properties of Finemet-type ribbons obtained by twin-roller melt-spinning," *Journal of Magnetism and Magnetic Materials*, vol. 322, pp. 3088-3093, 10// 2010.
- [17] N. S. Mitrovic, S. R. Djukic, and S. B. Djuric, "Crystallization of the Fe-Cu-M-Si-B (M=Nb, V) amorphous alloys by direct-current Joule heating," *IEEE Transactions on Magnetics*, vol. 36, pp. 3858-3862, 2000.
- [18] B. Ando, S. Baglio, V. Sacco, N. Savalli, and A. Bulsara, "Investigation on optimal materials selection in RTD-Fluxgate Design," in *2005 IEEE Instrumentation and Measurement Technology Conference Proceedings*, 2005, pp. 1261-1265.
- [19] K. Shirae, "Noise in amorphous magnetic materials," *IEEE Transactions on Magnetics*, vol. 20, pp. 1299-1301, 1984.



ISSN (Print) : 2320 – 3765
ISSN (Online): 2278 – 8875

International Journal of Advanced Research in Electrical, Electronics and Instrumentation Engineering

(An ISO 3297: 2007 Certified Organization)

Website: www.ijareeie.com

Vol. 6, Issue 6, June 2017

- [20] G. Hampel, A. Pundt, and J. Hesse, "Crystallization of Fe_{73.5} Cu₁ Nb₃ Si_{13.5} B₉ structure and kinetics examined by X-ray diffraction and Mossbauer effect spectroscopy," *Journal of Physics: Condensed Matter*, vol. 4, p. 3195, 1992.
- [21] H. Okumura, D. E. Laughlin, and M. E. McHenry, "Magnetic and structural properties and crystallization behavior of Si-rich FINEMET materials," *Journal of Magnetism and Magnetic Materials*, vol. 267, pp. 347-356, 12// 2003.
- [22] L. C. C. Benyosef, J. R. Teodósio, V. E. Taranichev, and B. V. Jalnín, "Improvements on CoFeSiB amorphous ribbon for fluxgate sensor cores," *Scripta Metallurgica et Materialia*, vol. 33, pp. 1451-1454, 1995/11/01 1995.